The Multi Aperture Scintillation Sensor (MASS) used in the site selection of the Thirty Meter Telescope (TMT)

S. G. Els, M. Schoeck, J. Seguel, W. Skidmore, D. Walker, et al.

S. G. Els, M. Schoeck, J. Seguel, W. Skidmore, D. Walker, A. Tokovinin, V. Kornilov, R. Riddle, T. Travouillon, E. Bustos, J. Vasquez, R. Blum, B. Gregory, P. Gillett, "The Multi Aperture Scintillation Sensor (MASS) used in the site selection of the Thirty Meter Telescope (TMT)," Proc. SPIE 7012, Ground-based and Airborne Telescopes II, 701222 (10 July 2008); doi: 10.1117/12.788954

SPIE.

Event: SPIE Astronomical Telescopes + Instrumentation, 2008, Marseille, France

The Multi Aperture Scintillation Sensor (MASS) used in the site selection of the Thirty Meter Telescope (TMT)

S.G. Els[a,b], M. Schöck[b], J. Seguel[a], W. Skidmore[b], D. Walker[a], A. Tokovinin[a], V. Kornilov[c], R. Riddle[b], T. Travouillon[b], E. Bustos[a], J. Vasquez[a], R. Blum[d], B. Gregory[a], P. Gillett[b]

[a]Cerro Tololo Inter-American Observatory, Casilla 603, La Serena, Chile;
[b]TMT Observatory Corporation, 2632 E. Washington Blvd., Pasadena, CA 91107, USA;
[c]Sternberg Astronomical Institute, Universitetsky prosp. 13, 119992 Moscow, Russia;
[d]National Optical Astronomy Observatory, 950 N. Cherry Ave., Tucson, AZ 85719, USA

ABSTRACT

One of the main tools used in the TMT site testing campaign is the turbulence profiler MASS. We describe empirical investigations and a side by side comparison of two MASS systems which were performed in order to identify the accuracy of MASS turbulence data and its dependence on the instrument calibration. The accuracy of the total seeing delivered by the TMT MASS systems is found to be better than 0"05. The combination of MASS and DIMM allows to observe the seeing within the first few hundred meters of the atmosphere and can be used to investigate possible correlations with meteorological parameters measured close to the ground. We also compare the detection of clouds and cirrus by means of MASS data (LOSSAM method) with measurements of the thermal emission of clouds using a net radiation sensor. These methods are compared with the visual cloud detection using all sky cameras.

Keywords: Site testing, instrumentation, turbulence profiling

1. INTRODUCTION

Over the past years the MASS turbulence profiler has evolved to one of the main tools for site testing and qualification works. Its measurement principle is based on the observation of the flying shadows which are caused by the incoming stellar light passing through turbulent layers of the atmosphere before hitting the entrance pupil of the telescope.[9] A unit which combines MASS and DIMM (Differential Image Motion Monitor[8]) instruments into a single instrument has been developed in recent years.[3] This rugged and compact device allows to measure most of the crucial turbulence parameters affecting astronomical observations; the vertical profile of the turbulence strength $C_n^2(h)dh$ is measured by the MASS at altitudes of $h = 0.5, 1, 2, 4, 8, 16$ km. From this profile the isoplanatic angle θ_0 and the seeing that would be seen by an observer located 500 m above the telescope pupil can be determined. In the following, we present a summary of a study addressing the precision of MASS results. We will also show that the combination of MASS and DIMM allows to investigate the evolution of the seeing within the first few hundred meters of the atmosphere. Finally, we will show a combination of different methods to detect the occurrence of clouds.

2. EXPERIMENTS ON THE MASS PRECISION

When the decision was taken to employ MASS turbulence profilers for TMT site testing, the precision of the instrument was only known rudimentary. It was therefore necessary to evaluate the precision which can be obtained by the MASS instrument. In the course of the TMT site testing project a variety of tests and experiments have been conducted to identify the precision of the MASS on empirical grounds. In the meantime, the MASS development team conducted theoretical studies which indicate that the MASS indeed delivers reliably the total turbulence strength.[9] Here, we give a condensed overview of the results of our empirical study which is described in more detail elsewhere.[2] In the following, the term *precision* is used for the difference between the medians of two observed statistical ensembles. While the *rms* of the turbulence measurements is dominated by the turbulence itself, the instrumental effects dominate the overall statistics of the data set.

Further author information: (Send correspondence to S.G.E.)
S.G.E.: E-mail: sels@ctio.noao.edu

Ground-based and Airborne Telescopes II, edited by Larry M. Stepp, Roberto Gilmozzi,
Proc. of SPIE Vol. 7012, 701222, (2008) · 0277-786X/08/$18 · doi: 10.1117/12.788954

Figure 1. Setup during the Tololo 2004 campaign. Two TMT site testing telescopes are installed on 6 m tall towers, close to the Northern edge of the Tololo summit platform. Picture courtesy of T. Travoullion.

2.1 Computational tests

The MASS processing software `turbina` allows in its later versions (since 2.052) a reprocessing of previously obtained data. The MASS results computed on the sites rely on the proper knowledge of the instrument settings prior to observation. The parameters of the MASS systems are the optical (system magnification and spectral response) and the detector electronical (Poisson parameter and non linearity) system settings. A thorough description of these parameters is given in [3] and [9]. In order to test the dependence of MASS results on these parameters, we conducted an empirical study. Using several months of real data observed at the TMT candidate sites, we reprocessed these data changing one parameter at a time and observing how the results change. It turns out that the detector response, the Poisson parameter, is of highest importance as it can change results by up to 0”06 if it is realistically but incorrectly chosen. We did not investigate how the combination of incorrect setup parameters would affect the results, however, we note that their individual impact can be of opposite sign. It is concluded that a good knowledge and monitoring of the MASS instrument setup is vital in order to obtain reliable results using the MASS instrument.

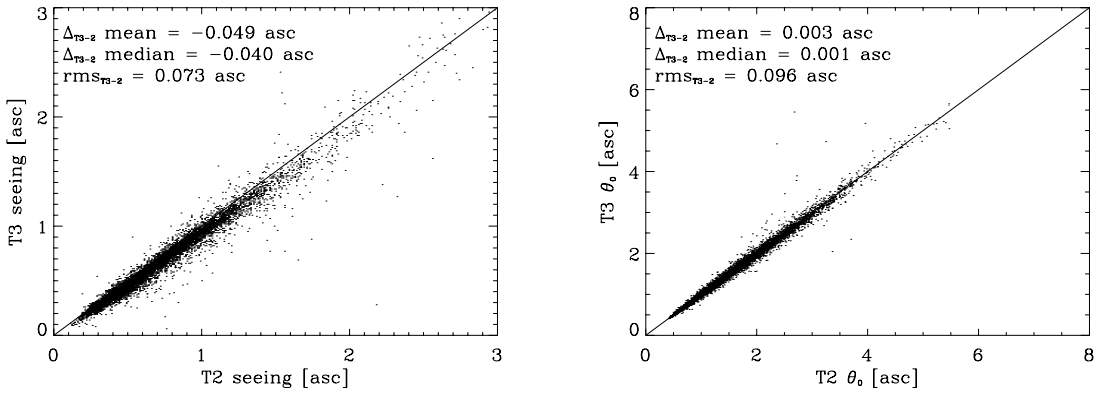

Figure 2. Comparison of MASS seeing (left) and isoplanatic angle (right) measurements by T2 and T3 obtained during the Tololo 2004 campaign. The numbers indicate the difference between the median (mean) values measured by the T2 and T3 systems. The rms is calculated around the 1:1 correlation. Figure as shown in [2].

2.2 The Tololo 2004 campaign

Between August and October 2004, the TMT site testing project had deployed two site testing telescopes, referred to as T2 and T3, on the summit of Cerro Tololo. All TMT site testing telescopes are Cassegrain telescopes with 35 cm aperture, custom built by Halfmann Teleskoptechnik GmbH. Both telescopes were mounted on 6 m tall towers, similar to the field setup on the candidate sites. The telescopes were horizontally separated by approximately 5 m. The setup on Cerro Tololo during the campaign is shown in Figure 1.

During the campaign both telescopes were observing the same stars during the same times. The automated data acquisition system (the robot) at each telescope triggered a MASS observation within one second of the DIMM observation. As a DIMM data acqusition cycle takes between 70 and 90 sec, MASS and DIMM data were only sampled at this rate. The data acquisition was not sychronized between the T2 and T3 systems, but as each system delivered a data point with the mentioned acqusition rate, the individual data points obtained by each system were typically separated by not more than 60 sec. The DIMM data obtained during this campaign have already been analysed earlier.[11]

The MASS data were reprocessed using `tubina (2.052)`[3] employing the correct instrument settings during the time of observation. The main results are shown in Figure 2. It is concluded that the precision of the seeing measured by the MASS devices is about 0"04. The very good precision which is found for the isoplanatic angle (better than 0"01) reflects the increasing agreement between the two systems at the higher $C_n^2(h)dh$ layers (above $h \sim 4$ km)[2] .

3. COMBINED MASS AND DIMM MEASUREMENTS: THE GROUND LAYER

As the MASS measures the seeing which would be seen by an observer located 500 m above the telescope and the DIMM provides a measurement of the total seeing from the entrance aperture to the top of the atmosphere, the combination of MASS and DIMM allows to obtain a measurement of the integrated turbulence strength within the first 500 m above the telescope. In the following, we will refer to these first 500 m as the ground layer (GL).

One of the main advantages of these GL seeing values is their high temporal sampling. In comparison, the acoustic turbulence profilers SODAR[10] provide turbulence profiles with a high vertical resolution up to several hundred meters above ground. However, these systems require typically about 20–30 minutes to obtain one of those profiles. Measurements of the turbulence strengths using either sonic anemometers or microthermal probes is in principle possible, but installing towers with a height of several hundered meters hosting these sensors – even though in principle possible – is impractical on the remote candidate sites.

Having a tool like the combined MASS-DIMM system for measuring the turbulence strength of the GL with good temporal sampling, one is tempted to investigate its connection with the physical conditions of the

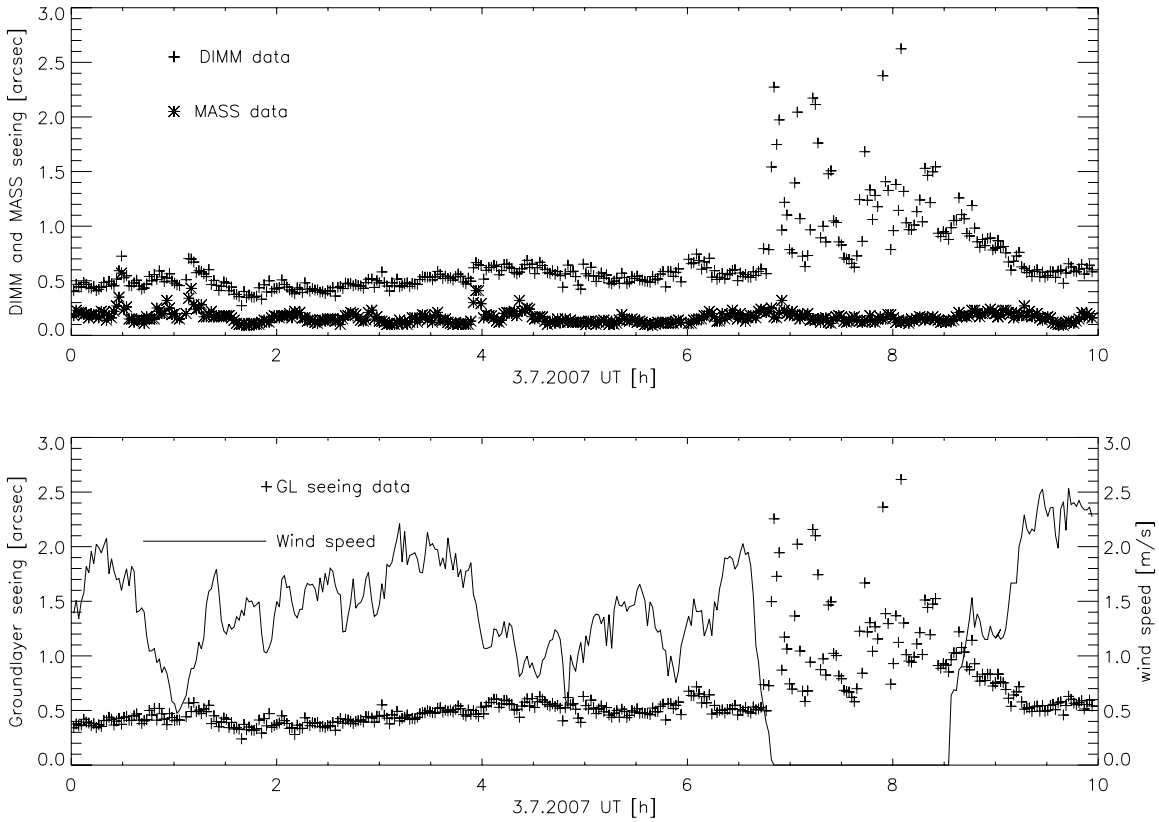

Figure 3. *Top:* MASS and DIMM measurements obtained at Cerro Armazones (T2) during the night of 02–03 July 2007. Note the strong increase of the DIMM seeing between about 7:00 and 8:30UT. *Bottom:* The ground layer seeing (GL) computed from MASS and DIMM during the same night. The solid line shows the wind speed. Note the drop to zero wind speed during the time of strong GL seeing.

atmosphere close to surface. A first attempt to look for correlations between general meteorological conditions at the site and the observed GL seeing has been reported earlier.[1] Back then it became clear that the energy balance between the surface and the atmosphere above is the crucial parameter. It was found that in several cases the quotient of wind speed and ground heat flux correlates with the evolution of the GL seeing. This is not a new finding; in boundary meteorology the theory describing the turbulence evolution over a flat surface is known as Monin Obukhov similarity theory. The parameter describing up to which altitude the turbulent energy production in the air is dominated by the mechanical interaction with the ground (friction) and not by thermal (buoyancy) forces, is the Monin-Obukhov length $L_\star$. It is given by

$$L_\star = -\frac{u^3 T \rho c_p}{\kappa g Q_H}, \tag{1}$$

where u is the friction velocity, T the air temperature, ρ the air density, c_p the heat capacity of air, g the gravitational acceleration and $\kappa = 0.4$ the von Kármán constant. The friction velocity u describes how the wind speed changes above a surface which shows a roughness with a typical size proportional to z_0. Using the measured wind speed $v(h)$ at an altitude h, the friction velocity is written as $u = v(h)/ln(h/z_0)$. The TMT site testing instrumentation includes also net radiation and ground heat flux sensors. These can be used to obtain the sensible heat flux, Q_H, in the above equation. Q_H is the difference between the ground heat flux and the net radiation. Therefore, all atmospheric parameters entering $L_\star$ are measured directly. Only the surface roughness z_0 requires an assumption on the typical size of surface features. In meteorology z_0 is typically set to values of

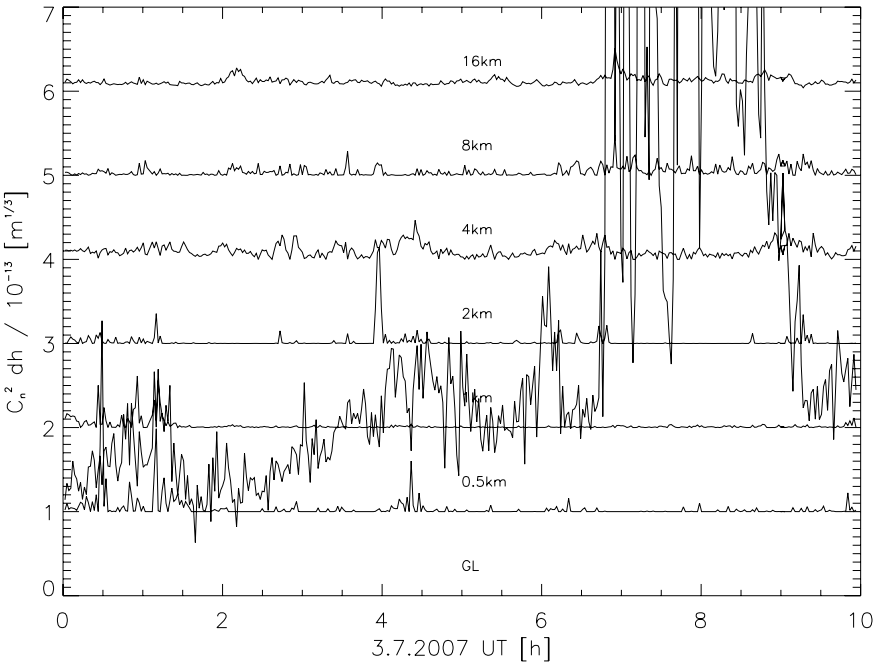

Figure 4. Individual MASS layer and ground layer (GL) turbulence strengths obtained at Cerro Armazones (T2) during the night from 02–03 July 2007. All values are normalized by 10^{-13}. The six MASS layers are shifted by (1, 2, ..., 6) in order to show the different layers. The (unshifted) GL is dominating the entire night and never drops below 10^{-13} $m^{1/3}$. No particular change in the strengths of the MASS layers is visible during the time in which the GL is very large (7–9 UT).

10%–30% of the true size of typical surface features. A brief study on a potential relationship between the GL seeing and $L_\star$ was shown in [1].

One of the concerns raised about correlating MASS-DIMM deduced GL seeing with wind speed is that the DIMM response depends on the speed with which the turbulent layers are swept over the two entrance apertures.[4] Investigations of this effect, show that the DIMM response function is correct only under very low wind speed conditions as averaging effects due to finite exposure times will not be significant in this regime[4,8]. This indicates that the DIMM measures turbulence also at zero wind speed, as long as the turbulence keeps changing the wave front above the DIMM entrance apertures. This movement can also be in the vertical direction, e.g., due to free convection of the atmosphere.

On the other hand the averaging effects decrease the response of the DIMM at non-zero wind speeds which then would mimic a decrease of the GL seeing. The TMT DIMM system does an extrapolation to zero exposure time using an exponential fit to six different exposure times.[11] Therefore, the influence of changing wind speeds on the aperture averaging should not play a role in the data presented here. In recent work,[9] it was shown that DIMM is intrinsically inaccurate for high-altitude turbulence and also the response of the DIMM depends on the optical quality of the DIMM images.[11] The combination of both dependences can lead to an over- as well as an underestimation of the total turbulence strength by the DIMM. We argue that, as the TMT DIMM instruments are monitored for their optical quality,[11] we can assume that abberation effects can be neglected.

The TMT DIMM systems employ ST-7 CCDs as detectors, which use a fan for cooling of the CCD. So the increased DIMM seeing might be caused by the ST-7 "cooling jet" which introduces turbulence either inside the instrument or in the telescope tube. The first option is unlikely as the MASS-DIMM instrument is well sealed and the fan is directing its flow away from the instrument. The later option could be possible as the TMT site testing telescopes are an open tube design and one could imagine the (warm) air flow from the ST-7 fan

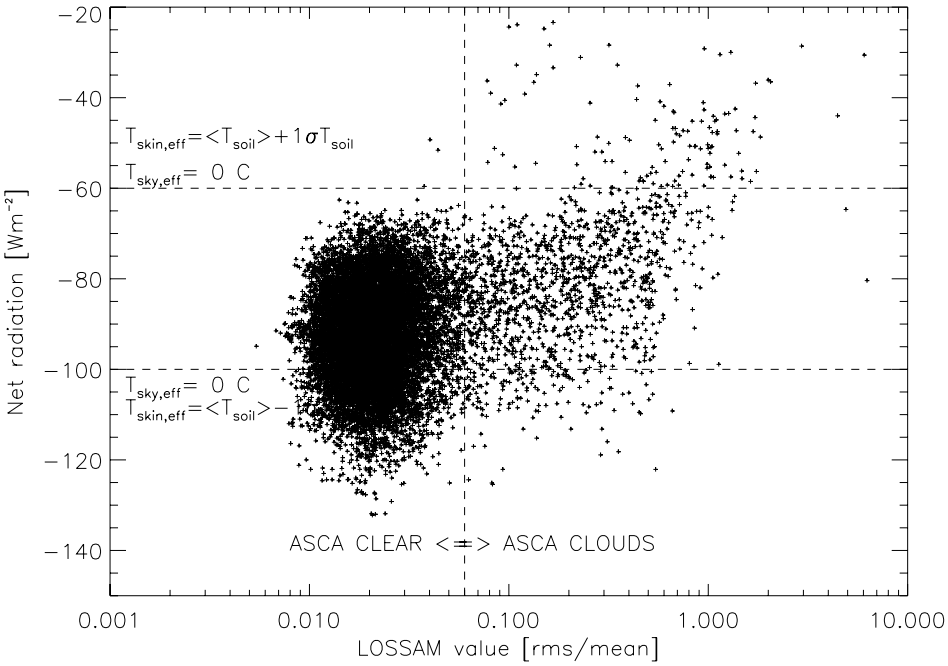

Figure 5. Comparison of net radiation measurements and MASS LOSSAM observations taken at Cerro Armazones.

to go around the primary mirror support structure and entering the optical path of the telescope. However, we note that there are other site testing programmes which use a closed tube DIMM telescope, which also observe increases in the GL seeing during periods of low wind speeds.[7] This indicates that the effect of enhanced GL is not attributable to the "cooling jet" of the ST-7 CCD.

There remains the possibility that low wind speed conditions occur when the turbulence profile is taking a particular shape which favors the DIMM to overestimate the true seeing. In Figure 3, the occurrence of strong GL seeing during a single night observed at Cerro Armazones is shown. It can be seen that the increased DIMM seeing coincides with zero wind speed. In Fig. 4 the turbulence strength of the individual MASS layers of that night is shown. No particular behaviour of the layers can be seen during the time between 7 and 9 UT. In this time span the GL seeing increases significantly but the higher MASS layers do not show any particular change as compared to the rest of that night.

From all this we conclude that the MASS-DIMM based observations showing an increase of the GL seeing under low wind speed conditions are in fact indicating the occurrence of free convection in the atmosphere and are not an instrumental artefact.

4. CLOUD DETECTION USING NET RADIATION SENSORS

The TMT site testing program employs all sky cameras for the detection of clouds.[6] As mentioned above, the TMT site testing equipment includes net radiation sensors. These sensors are the Middleton Solar CN1-R Net Pyrradiometer. They consist of a double sided thermopile bonded between two thin aluminum plates. The coating of these aluminum plates shows a flat spectral response from 0.3μm to 60μm. The sensor is sealed inside a polythene dome. The incident radiation from the sky or ground is absorbed by either the upper or lower sensor plate, resulting in an elevation of the temperature of the corresponding plate. This results in a temperature gradient between upper and lower junctions of the thermopile, whose output is then proportional to the difference between the upper and lower irradiance ($R_{\rm net}$). The sensor is sensitive to radiation from 4π steradian.

As these sensors are sensitve into the far infrared they could, in principle, be used to detect clouds, by means of the thermal emission of the aerosols. The radiation equation at the ground is given by $Q_{\rm rad} = I_\downarrow + I_\uparrow + K_\downarrow + K_\uparrow$ where I refers to the infrared and K to the short wavelength radiation. The components originating from the sky are marked as $\downarrow$ and are directed towards the ground. Upward radiation is marked by $\uparrow$ and originates from the ground. During the day, $K_\downarrow$ is dominated by solar radiation and due to the ground albedo α, its reflected part forms $K_\uparrow$. At night time, the K components can be assumed $K_\uparrow = K_\downarrow \approx 0$ (the effect of radiation from the moon is not detected by the net radiation sensors). Therefore, during night time the net radiation sensors measure only $R_{\rm net} = I_\downarrow - I_\uparrow$. In the following, $R_{\rm net} = Q_{\rm rad}$ is used occasionaly.

The IR radiation $I_\downarrow$ is created mainly by thermal emission from molecules and aerosols in the atmosphere above the site. It can be expected that above a certain concentration of aerosols or water vapour, clouds or cirrus will form and increase $I_\downarrow$. As during the TMT site testing neither $I_\downarrow$ nor $I_\uparrow$ are measured independently, it is necessary to obtain information on $I_\uparrow$ to remove the impact of changes of the soil temperature on $R_{\rm net}$. The thermal emission from the ground surface, or skin, is

$$I_\uparrow = \sigma T_{\rm eff,skin}^4. \tag{2}$$

The problem is that $T_{\rm eff,skin}$ is not known. Also the $T_{\rm eff,skin}$ is affected by various factors, for example wind gusts can cool the surface quickly.

On the TMT candidate site Cerro Armazones in northern Chile, a soil temperature sensor is deployed since early 2007. No strong variations of the recorded $T_{\rm soil}$ are observed and the night time soil temperature at a depth of $z \sim 10$ cm is $T_{\rm soil} = 15.4 \pm 3.4$°C. Using Eq. (2) and assuming that $T_{\rm eff,skin} = T_{\rm soil}$ results in an average $I_\uparrow \approx 393 \pm 19$ Wm^{-2}. Assuming that the sky radiates, under the presence of clouds, with $T_{\rm sky,eff} = 0$°C, results in a threshold for clouds in the net radiation of $R_{\rm rad,clouds} > -96... - 60$ Wm^{-2}. It is, however, not possible to use these numbers alone as the threshold for the appearance of clouds. $T_{\rm sky,eff}$ is very complex: clouds show patchy appearance changing the "filling factor" (the fraction of the sky covered by the cloud), they also appear at various altitudes lowering or raising the aerosol temperature.

Nevertheless, these numbers are tested against observations in Fig. 5. The Line Of Sight Sky Absorption Monitor (LOSSAM)[5] is a method which correlates the quotient of the observed stellar flux and its variation to the sky opacity. Comparison between MASS based LOSSAM values and all sky camera (ASCA) observations have shown that a LOSSAM value of ∼0.06 can be used as threshold for the occurrence of clouds.[6] We adopt this value here and it can be seen that indeed for net radiation values $R_{\rm rad,clouds} > -60$ Wm^{-2} clouds are detected by all three methods. It has to be noted that Fig. 5 is only based on simultaneous MASS and net radiation observations. As the robotic system shuts down if the flux variation becomes too large, no MASS data are available when the sky becomes cloudy along the line of sight of the telescope. The region between -96 and -60 Wm^{-2} in which LOSSAM> 0.06 is most likely dominated by the patchy occurence of clouds. The region below -100 Wm^{-2} is the region in which cold cirrus or high altitude clouds are causing LOSSAM cloud detections.

The main problem of using the net radiation for reliable cloud detection is to overcome the variability of the ground emission. One method to achieve that goal could be based on the comparison of the variability of the net radiation measurement with the ground heat flux variation within certain time bins. In Fig. 6 and Fig. 7 we show two nights of cloud occurrence above Cerro Armazones as observed by the all sky camera.[6] The top panel shows the observed net radiation and ground heat flux measurements, as well as the variability of the net radiation in 30 min bins. This time binning was chosen as it was found that it takes several minutes before a cooling event (wind gusts) is penetrated into the ground to the depth of the ground heat flux sensor. It appears that the combination of ground heat flux and net radiation measurements can be used to trace the occurrence of clouds. A thresholding scheme is proposed in which the variability and absolute number of the net radiation, compared to the variability of the ground heat flux are used to flag the time periods of clouds.

Thick, low (warm) clouds, however, can be detected if the net radiation value reaches the level of the emission expected by liquid aerosols. All this is work in progress and because clouds are detected by two other methods in the TMT site testing program,[6] it will be possible to properly calibrate the net radiation measurements using these methods.

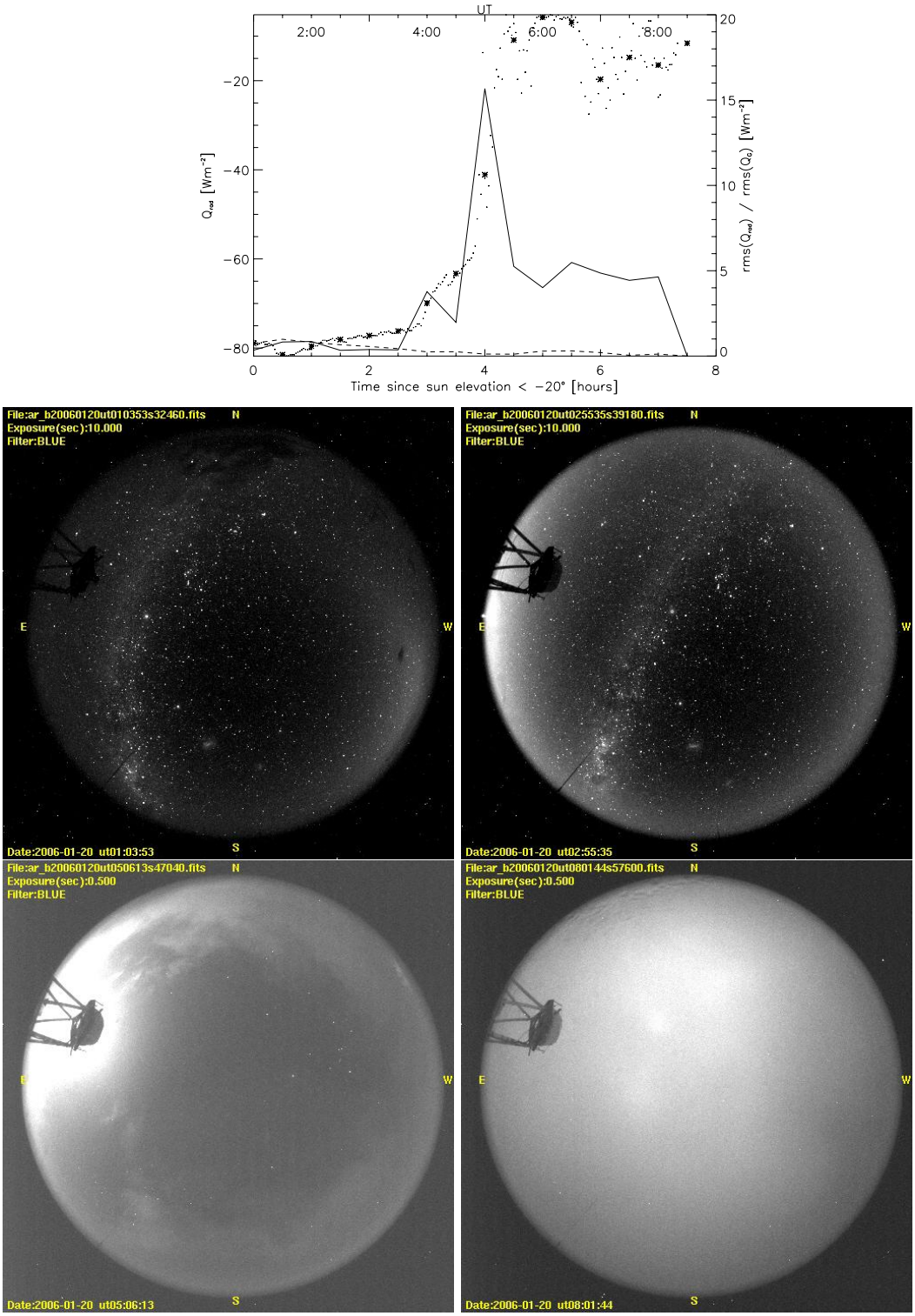

Figure 6. The night of 19-20 January 2006 on Armazones. **Top panel:** $Q_{\rm rad}$ data are shown as dots. The asterisks indicate the 30 min. mean values. The solid line shows the $rms(Q_{\rm rad})$ and the dashed line the $rms(Q_{\rm G})$ in the 30 min bins. **The panels below** show B band ASCA images during that night. **Middle, left:** UT 01:03:53, B filter shows a few clouds. **Middle, right:** UT 02:55:35, clear sky. **Bottom, left:** UT 05:06:13, thick clouds appear. **Bottom, right:** UT 08:01:44, overcast, fog?

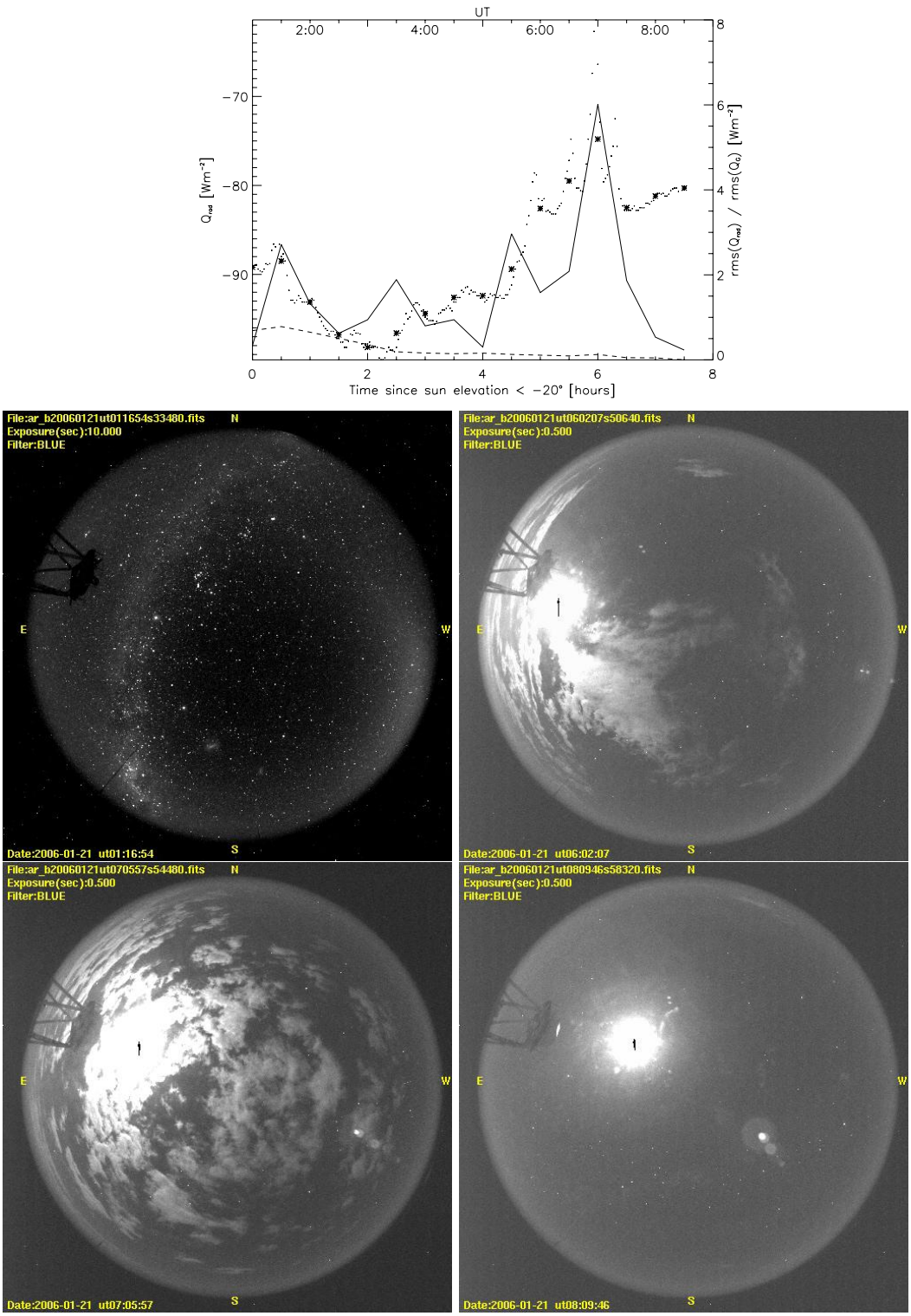

Figure 7. The night of 20-21 January 2006 on Armazones. **Top panel:** $Q_{\rm rad}$ data are shown as dots. The asterisks indicate the 30 min. mean values. The solid line shows the $rms(Q_{\rm rad})$ and the dashed line the $rms(Q_{\rm G})$ in the 30 min bins. **The panels below** show B band ASCA images during that night. **Middle, left:** UT 01:16:54, B filter shows clear sky, but the R filter shows some haze like structure. **Middle, right:** UT 06:02:07, first clouds appear. **Bottom, left:** UT 07:05:57, clouds/cirrus at zenith. **Bottom, right:** UT 08:09:46, clouds passed, sky mostly clear.

5. SUMMARY

The general precision of the MASS turblence profiler was presented. The combination of simultaneous MASS and DIMM observations also allows to measure the GL seeing within the first 500 m above the surface. Evidence was shown that that GL investigations can be done with reasonable accuracy even with the recently identified problems of the DIMM response. Finally, an investigation of the use of net radiation measurements for cloud detection was presented.

ACKNOWLEDGMENTS

We are greateful to Hugo E. Schwarz for his work on the development of the all sky camera systems and for pointing out the potential use of a net radiation sensor for the detection of clouds. We thank the Cerro Tololo Inter-American Observatory staff for their support and hospitality. The TMT Project gratefully acknowledges the support of the TMT partner institutions. They are the Association of Canadian Universities for Research in Astronomy (ACURA), the California Institute of Technology and the University of California. This work was supported as well by the Gordon and Betty Moore Foundation, the Canada Foundation for Innovation, the Ontario Ministry of Research and Innovation, the National Research Council of Canada, the Natural Sciences and Engineering Research Council of Canada, the British Columbia Knowledge Development Fund, the Association of Universities for Research in Astronomy (AURA) and the U.S. National Science Foundation.

REFERENCES

[1] Els S.G., Vogiatzis K., "Revealing the onset of free convection in terrestrial planet atmospheres", in 'Convection in Astrophysics', Proc. IAU Symp. 239, 2006, Eds. F. Kupka, I. Roxburgh and K. Chan, pp.172-174

[2] Els S.G., Schöck M., Seguel J., et al., "Study of the precision of the Multi Aperture Scintillation Sensor turbulence profiler employed in the site testing campaign for the Thirty Meter Telescope", 2008, Appl. Optics, *47*, 14, 2610

[3] Kornilov V., Tokovinin A., Shatsky N., et al., "Combined MASS-DIMM instruments for atmospheric turbulence studies", 2007, MNRAS, *382*, 1268

[4] Martin H.M., "Image motion as a measure of seeing quality", 1987, PASP, *99*, 1360

[5] Sarazin M., see `http://www.eso.org/gen-fac/pubs/astclim/lasilla/asm/lossam/rationale.html`

[6] Skidmore W., Schöck M., Magnier E., et al., 2008, SPIE, *this conference*

[7] Thomas-Osip J.E., et al., 2008, SPIE, *this conference*

[8] Tokovinin A., "From Differential Image Motion to Seeing", 2002, PASP, *114*, 1156

[9] Tokovinin A., Kornilov V., "Accurate seeing measurements with MASS and DIMM", 2007, MNRAS, *381*, 1179

[10] Travouillon T., "SODAR calibration for turbulence profiling in TMT site testing", 2006, SPIE, 6267, 65

[11] Wang L., Schöck M., Chanan G., et al., "High-accuracy differential image motion monitor measurements for the Thirty Meter Telescope site testing program", 2007, Appl. Optics, *46*, 25, 6460